Glass quantization of the Gaussian core model

Jean-Marc Bomont,[1] Christos N. Likos,[2] and Jean-Pierre Hansen[3,4]
[1]*Université de Lorraine, LCP-A2MC, UR 3469, 1 Blvd. François Arago, Metz F-57078, France*
[2]*Faculty of Physics, University of Vienna, Boltzmanngasse 5, 1090 Vienna, Austria*
[3]*PHENIX, Sorbonne Université, F-75005 Paris, France*
[4]*Department of Chemistry, University of Cambridge, Cambridge CB2 1EW, United Kingdom*

(Received 23 November 2021; revised 24 January 2022; accepted 7 February 2022; published 22 February 2022)

We use the replica method to study the dynamical glass transition of the Gaussian core model, a system of ultrasoft repulsive spheres interacting via a Gaussian potential, focusing on low temperatures and low-to-moderate densities. At constant temperature, an amorphous glassy state is entered upon a first compression but this glass melts as the density is further increased. In addition to this reentrant transition, a second, smooth transition is discovered between a continuous and a discretized glass. The properties of the former are continuous functions of temperatures, whereas the latter exhibits a succession of stripes, characterized by discontinuous jumps of the glassiness parameters. The glass physics of ultrasoft particles is hence richer than that of impenetrable particles for reasons that can be attributed to the ability of the former to create and break out-of-equilibrium clusters of overlapping particles.

DOI: 10.1103/PhysRevE.105.024607

I. INTRODUCTION

Interactions between particles of simple atomic liquids are usually modeled by pair potentials with a strongly repulsive component, diverging at short range. An emblematic model in statistical physics for the study of hard colloids [1] is the hard sphere system whose density-driven fluid-solid and fluid-glass transitions have been extensively studied. Contrasting with such hard-core systems, there has been much recent interest in studying experimentally colloidal systems composed of ultrasoft particles [2,3]. In particular, soft colloids can overlap and deform and may thus be compressed up to packing fractions that cannot be reached with hard particles. As a result, the physics of ultrasoft particles is richer than that of hard ones [4,5], exhibiting striking anomalies, such as nonmonotonic density dependence of the freezing transition [6] or complex cascades of cluster crystalline states [7–9].

A widely examined ultrasoft system is the Gaussian core model (GCM), introduced by Stillinger [10–12], for which the pair-interaction reads

$$v(r) = \varepsilon \exp[-(r/\sigma)^2], \tag{1}$$

where ε and σ are energy and length scales. From these two variables, a reduced density $\rho^* = \rho\sigma^3$ and a reduced temperature $T^* = k_B T/\varepsilon$ can be defined, where $\rho = N/V$ is the number density, k_B is Boltzmann's constant, and T the absolute temperature. The GCM was originally proposed as an effective potential of interaction between self-avoiding polymer coils by Flory and Krigbaum [13]. Subsequent work by Grosberg *et al.* [14] established, on the basis of scaling arguments arising from polymer connectivity, that the correct scaling of the amplitude ε with the degree of polymerization M is $\varepsilon \sim M^0$, i.e., the amplitude is independent of the molecular weight. Louis *et al.* [15–17] derived accurate effective potentials between polymer coils at various concentrations, confirming both the Gaussian form of the interaction and the independence of its amplitude on M in the limit $M \gg 1$. Furthermore, Götze *et al.* [18] showed that the GCM is also materialized as an effective interaction between flexible dendrimers, the amplitude being tunable through the number of generations of the latter. Stillinger *et al.* [10–12] carried out a wealth of detailed theoretical investigations on the phase behavior of the GCM, focusing in particular in the low-temperature regime. Since their pioneering work, which has been later confirmed and elaborated by complementary numerical investigations, it is known that the GCM exhibits, at equilibrium, a reentrant fluid-solid-fluid phase diagram under compression below a threshold upper freezing temperature $T_u^* = 8.74 \times 10^{-3}$, above which it remains fluid at all densities [6,19,20].

In previous work, Ikeda and Miyazaki [21,22] investigated numerically the dynamical properties of the supercooled states of the GCM, finding that nucleation is suppressed and that mode-coupling theory provides an accurate description of the slow dynamics at high densities. In the present paper, we investigate the ways in which the complex equilibrium phase diagram of the ultrasoft GCM also impacts its transition to glassy states. Our main finding is an unexpected density dependence of the glassy behavior of ultrasoft GCM particles. On one hand, a reentrant glass formation follows the behavior observed for equilibrium crystallization, arising from the mean-field character of the GCM at high densities [6,16,23,24]; on the other hand, at moderate densities, a quantized glass emerges, where the characteristic order parameters at constant density undergo sudden jumps upon varying the temperature, and thus organize in stripes. Within each stripe glassiness is "frozen," a property resulting from the formation of out-of-equilibrium clusters, which require sufficient

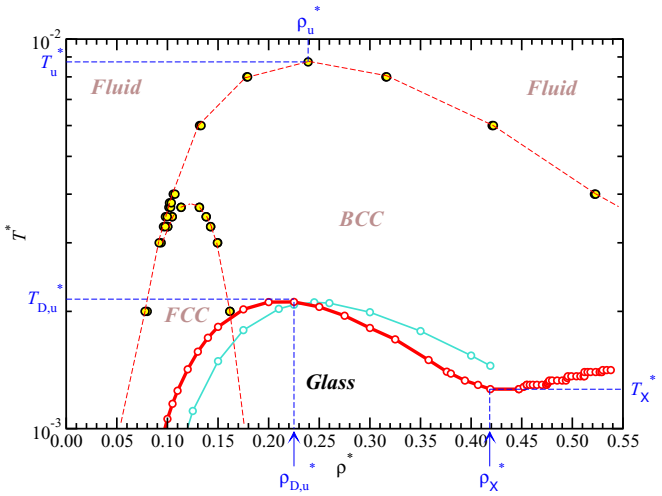

FIG. 1. Glass and equilibrium phase diagrams of the Gaussian core model. The full red line signals a dynamical transition between a (supercooled) fluid above and a glass below. The turquoise line shows the dependence of Kauzmann temperature T_K^* on density ρ^*. The blue broken lines pinpoint three characteristic pairs of state points discussed in the text. The yellow-filled circles denote equilibrium phase boundaries between the labeled phases, as calculated by computer simulations in Ref. [19] (courtesy of S. Prestipino). The broken red lines connecting these points are guides to the eye.

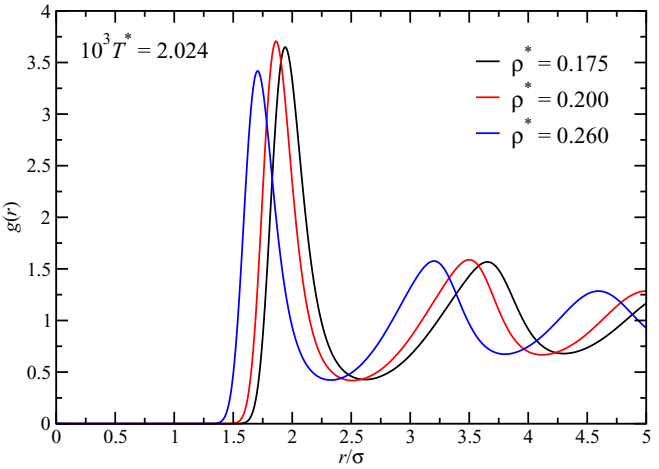

FIG. 2. Reentrant behavior of the glass RDF $g(r)$ at reduced temperature $T^* = 2.024 \times 10^{-3}$ for three densities ρ^* listed above.

thermal agitation to break up. Moving along the density axis in each stripe results in a smooth dependence of glassiness on concentration. Overall, upon compressing the system at constant temperature, the GCM undergoes a second-order transition from a continuous to a quantized glass.

The rest of the paper is organized as follows. In Sec. II, we briefly review the essentials of the replica theory approach to dynamical arrest. In Sec. III we present our main result on the glassy states of the GCM and in Sec. IV we analyze in detail the interparticle correlations in the quantized glass state. Finally, in Sec. V, we summarize and draw our conclusions.

II. REPLICA THEORY APPROACH TO THE GLASS TRANSITION

We follow an idea borrowed from spin glass theory [25–28], by considering two copies (replicas) of our system, coupled by a weak, short-range inter-replica attraction, chosen to be of the form

$$\beta v'(r,c) = -\varepsilon_{12}\left[\frac{c^2}{r^2+c^2}\right]^6 = -\varepsilon_{12} w(r,c), \qquad (2)$$

with a coupling constant $\varepsilon_{12} \geqslant 0$. The range parameter c, which must be of the order of or smaller than the typical interparticle distance $a \sim \rho^{-1/3}$, is fixed at the value 0.3σ to ensure that an atom of one replica can interact at most with one atom of another replica. The exact form of the chosen $w(r,c)$ is irrelevant, since we shall be interested in the limit $\varepsilon_{12} \to 0$. The order parameter of the liquid-glass transition is the mean overlap between copies,

$$Q = 4\pi\rho \int_0^\infty g_{12}(r) w(r,c) r^2 dr, \qquad (3)$$

where $g_{12}(r)$ is the radial distribution function (RDF) between the two copies. The pair structure of such a symmetric binary mixture is characterized by the intrareplica RDF $g_{11}(r) = g_{22}(r) \equiv g(r)$ and its aforementioned inter-replica counterpart $g_{12}(r)$. In the liquid phase, $g_{12}(r)$ is equal to 1 and Q reduces to its "random overlap value" Q_R. In the glass phase, $g_{12}(r)$ has a nontrivial structure, reminiscent of the radial distribution function of a liquid, but with an additional peak at $r = 0$, such that strong intercopy correlations imply that $Q \gg Q_R$ in the glass phase.

We have solved the coupled hypernetted chain (HNC) integral equations [29] for $g(r)$ and $g_{12}(r)$ along several isochores ranging from $\rho^* \cong 0.1$ up to $\rho^* \cong 0.53$. The HNC closure has been shown to be very accurate for the GCM [6,16], and more generally for bounded potentials [30], in particular by detailed comparisons with numerical simulations [6,16]. The HNC closure becomes exact in the high density limit, despite a lack of full thermodynamic consistency [31]. For each ρ^*, on gradually lowering the temperature, if ε_{12} is initially set to zero, the two copies are completely decoupled and trivially $g_{12}(r) = 1$ and $Q = Q_R$. The system reduces to two independent, identical supercooled liquids. At variance, on lowering the temperature for an initial nonzero value of the coupling, long-range correlations develop with an emerging peak close to $r = 0$ in $g_{12}(r)$, whose amplitude grows as T decreases, indicating that copies gradually correlate. At some sufficiently low temperature, both order parameters undergo a discontinuous jump to much higher nontrivial values, which persist even when ε_{12} is progressively switched off. This jump signals a broken replica symmetry of the system, a feature that constitutes the very foundation of the replica method [28]. On the contrary, if ε_{12} is switched off too hastily, initially paired atoms drift away from each other in the supercooled liquid phase. In the present scenario, ε_{12} was progressively lowered from its initial value, namely $\varepsilon_{12}^0 = 0.01\varepsilon$ with $c = 0.3\sigma$, until extinction and the corresponding nontrivial $g_{12}(r)$ was used to calculate the corresponding overlap Q. In order to map out the glass phase diagram within this range of densities, we searched for the highest temperature, $T_D^*(\rho^*)$, at which a nontrivial Q value survives for a given density. To achieve

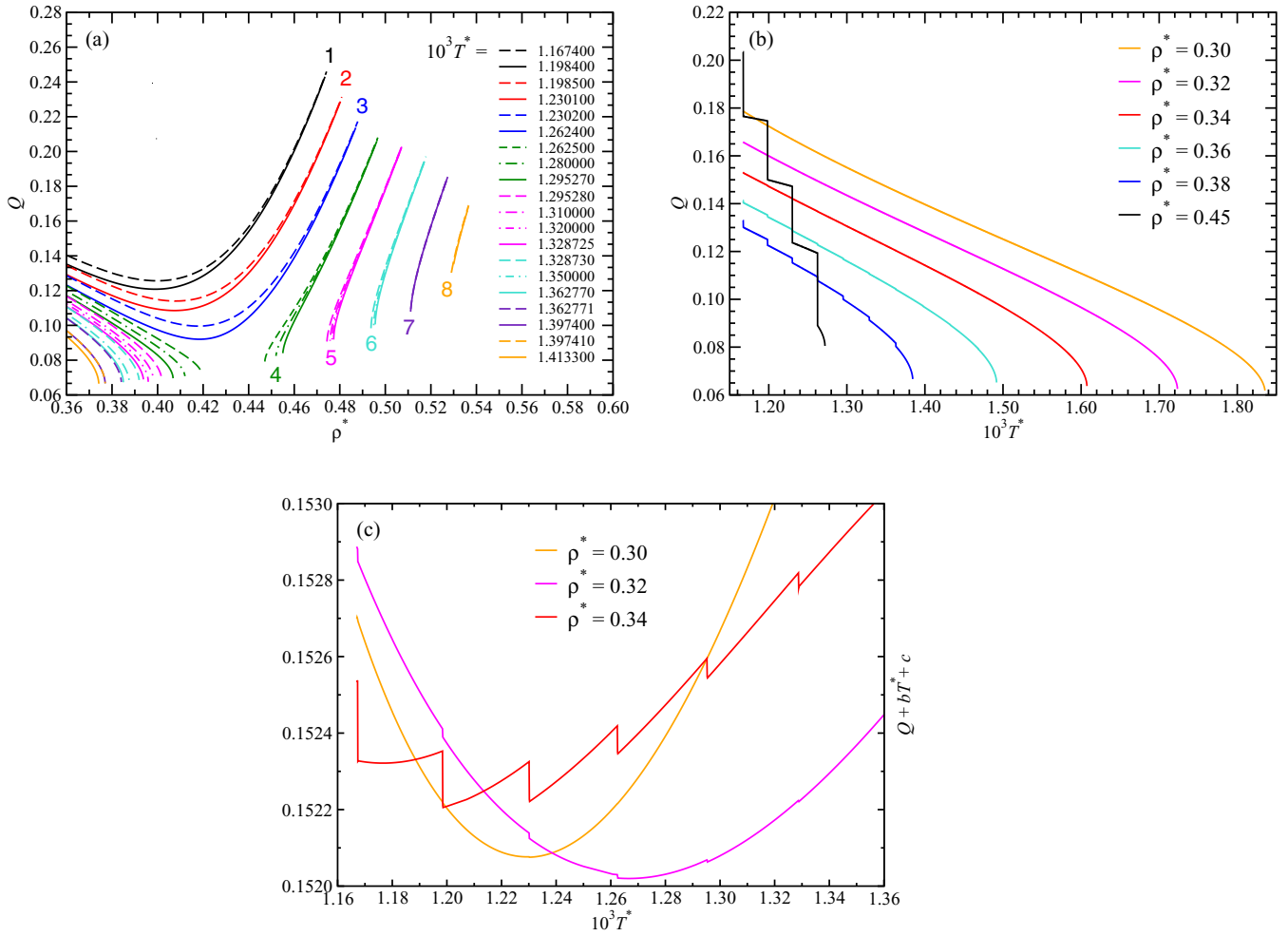

FIG. 3. (a) Overlap parameter Q as a function of density, along various isotherms specified on the right. The numbers label the eight detected stripes, starting from the lowest temperature explored. (b) The overlap parameter Q as a function of temperature along the labeled isochores. (c) A zoom on the Q-vs-T^* curves of panel (b) for the three lowest densities in that panel; a straight line $bT^* + c$ has been added to Q, to render the tiny jumps between stripes visible for the two highest densities. The arbitrary parameters b and c depend on ρ^* and have been determined to enhance visibility.

this, each state, described by the triplet (ρ^*, T^*, Q), was annealed. It is worth noting that, in a purely static framework, $T_{\rm D}^*(\rho^*)$ is equivalent to the ideal mode coupling dynamical transition [32].

III. GLASSY STATES OF THE GAUSSIAN CORE MODEL

The numerical $T_{\rm D}^*(\rho^*)$ values obtained by the method outlined above are reported in Fig. 1. We notice the existence of a crossover density $\rho_\times^* = 0.4184$, associated with a temperature $T_\times^* = 1.2624 \times 10^{-3}$, and an upper dynamical transition temperature $T_{\rm D,u}^* = 2.115 \times 10^{-3}$, associated with density $\rho_{\rm D,u}^* = 0.225$. For $\rho^* \geqslant \rho_\times^*$, the dynamical transition line features characteristic steps, whereas for $\rho^* < \rho_\times^*$ it exhibits a reentrant shape reminiscent of the form of the equilibrium freezing line, in agreement with previous findings for Hertzian spheres [33,34] or star polymers [35]. For temperatures $T^* \geqslant T_{\rm D,u}^*$, to be compared to the highest equilibrium freezing temperature $T_{\rm u}^* = 8.74 \times 10^{-3}$ [19], the GCM does not vitrify under any compression. The corresponding density $\rho_{\rm D,u}^* = 0.225$ is very close to the density $\rho_{\rm u}^* = 0.239$ where the equilibrium freezing transition line reaches its maximum. This feature is reflected in the reentrant dependence of the height of the main peak of the glass $g(r)$ with density at fixed temperature, in full analogy with its liquid counterpart [6], as shown in Fig. 2.

Since in the supercooled liquid phase the two copies are uncorrelated when $\varepsilon_{12} = 0$, the calculation of thermodynamic and structural properties can be carried out on the one-component (single copy) system. The free energy divides into ideal and excess parts, $f_{\rm id}(\rho^*, T^*)$ and $f_{\rm ex}(\rho^*, T^*)$, respectively. In the deeply supercooled liquid phase, atoms are trapped over long periods in nearest neighbor cages, the order of magnitude of the residence time in these cages being given by the Maxwell relaxation time $\tau_{\rm M} = \eta/G_\infty$, with the viscosity η and the shear modulus G_∞ of the fluid. It is therefore natural to split the free energy into configurational and vibrational components, $f_{\rm c}(\rho^*, T^*)$ and $f_{\rm v}(\rho^*, T^*)$, respectively, where the latter is determined by the mean vibration frequency ω_0 in a disordered medium, set by the mean square force acting on an atom. Knowledge of $f_{\rm ex}$ allows then the calculation of the configurational free energy via $f_{\rm c}(\rho^*, T^*) = f_{\rm ex}(\rho^*, T^*) + f_{\rm id}(\rho^*, T^*) - f_{\rm v}(\rho^*, T^*)$. The Kauzmann tem-

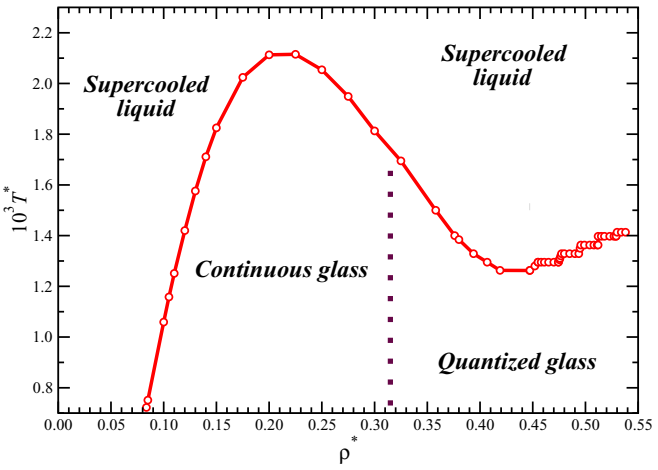

FIG. 4. Glass phase diagram of the Gaussian core model calculated as explained in the main text. Below the red vitrification line, two states, namely a continuous glass and a quantized glass, appear, separated by a continuous transition line along the critical isochore $\rho_c^* = 0.315$.

perature $T_K(\rho^*)$ is defined as the T value at which the configurational entropy $s_c = S_c/(Nk_B)$ vanishes, i.e.,

$$s_c = -\left(\frac{\partial f_c^*}{\partial T^*}\right)_{\rho^*, T^* = T_K^*} = 0, \tag{4}$$

where $f_c^* = T^* f_c$; at T_K^*, $f_c^*(\rho^*, T^*)$ goes through a maximum along an isochore. Independently of the replica method, we have furthermore calculated the Kauzmann temperature [36] $T_K(\rho^*)$ along several isochores, within the Einstein solid approximation [37]. The $T_K(\rho^*)$ line, shown in Fig. 1, also points to a reentrant glass phase, but with a shift in density compared to the $T_D(\rho^*)$ line.

The crossover point $(\rho_\times^*, T_\times^*)$ in Fig. 1 exhibits a local minimum of the dynamical transition line. Accordingly, and for $T^* \leqslant T_\times^*$, the overlap parameter Q first decreases with density along an isotherm up to $\rho^* = \rho_\times^*$ and then it increases again. The same quantity displays a gap for $T^* \gtrsim T_\times^*$, since the supercooled liquid separates two glassy regions. The dependence of Q on ρ^* along various isotherms is shown in Fig. 3(a). On the high-density side, and although the temperature increases continuously, Q no longer varies continuously, but one rather observes that the curves $Q(\rho^*)$, drawn in the same plot for different temperatures, now bundle together to form well-defined stripes. Within the range of temperatures we explored, we were able to identify eight such stripes, and we anticipate that their presence will also persist at lower temperatures. Each of these stripes, labeled by the index i, is well defined over a range of temperatures $[T_{\min,i}^*, T_{\max,i}^*]$ and its own range of densities, $[\rho_{\min,i}^*, \rho_{\max,i}^*]$. If a state point (ρ^*, T^*, Q) within stripe i is gradually annealed within the temperature range $[T_{\min,i}^*, T_{\max,i}^*]$, Q does not vary or it does so only infinitesimally. In passing from stripe i to stripe $i+1$, for which $T_{\min,i+1}^* = T_{\max,i}^*$ holds, the overlap Q undergoes a discontinuous jump, indicating that in order to pass from one stripe to the next, the system requires a finite amount of thermal energy. Note that, as i increases, the amplitude in density, $\rho_{\max,i}^* - \rho_{\min,i}^*$, decreases, suggesting a layered structure of the glass stability domain in the (ρ^*, T^*) plane for $\rho^* > \rho_\times^*$. The highest layer in terms of temperature was identified for $T^* = 1.4133 \times 10^{-3}$.

The dependence of Q on temperature along different isochores is shown in Fig. 3(b), where the existence of stripes becomes obvious. At the lower densities, the dependence of Q on T^* appears continuous, whereas jumps between stripes of increasing size are visible as density grows beyond $\rho^* = 0.36$. To localize the onset of such jumps more clearly, we plot in Fig. 3(c) the quantity $Q + bT^* + c$ against T^* with suitably chosen, ρ^*-dependent parameters b and c, revealing that, while the curves are continuous for $\rho^* = 0.30$, tiny jumps show up already for $\rho^* = 0.32$. Accordingly, we estimate the critical density $\rho_c^* = 0.315$ as the point at which a transition in the nature of the glass occurs: whereas no stripes are present for $\rho^* \leqslant \rho_c^*$, they appear at this threshold, with a gap between successive stripes whose size grows continuously with ρ^* for $\rho^* > \rho_c^*$. Consequently, the dynamical phase diagram of the

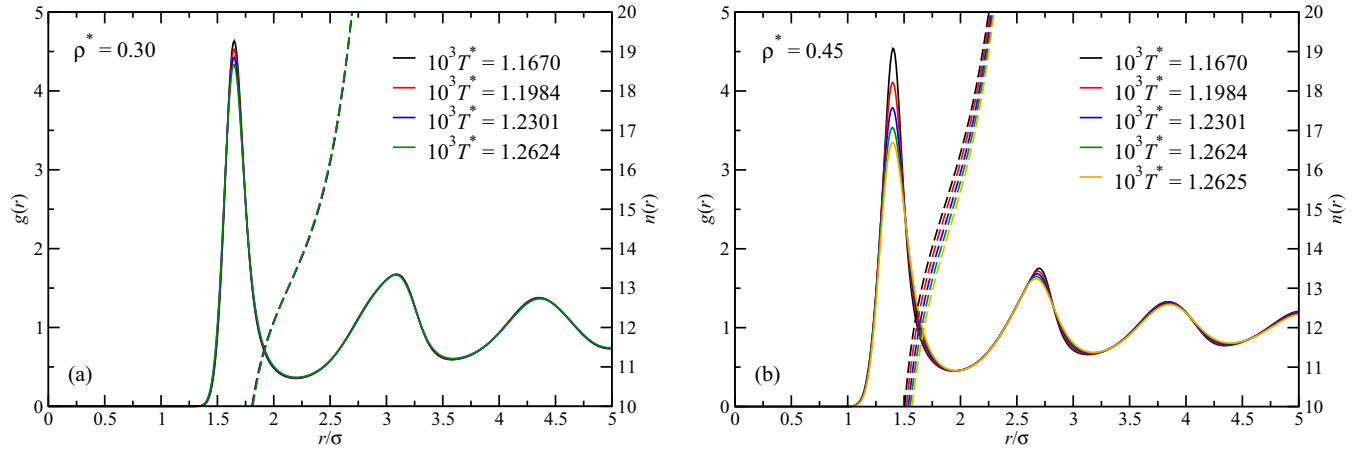

FIG. 5. (a) Radial distribution function $g(r)$ of the glass (solid lines, vertical axis to the left) and number of neighbors $n(r)$ at a distance r from a given particle in the glass (broken lines, vertical axis to the right) at various temperatures, specified above, at density $\rho^* = 0.30$, where glassiness is predicted to be continuous. (b) Same as in panel (a) but at density $\rho^* = 0.45$, where glassiness is predicted to be quantized. In both panels, the $g(r)$ and $n(r)$ curves are color matched at each temperature under consideration.

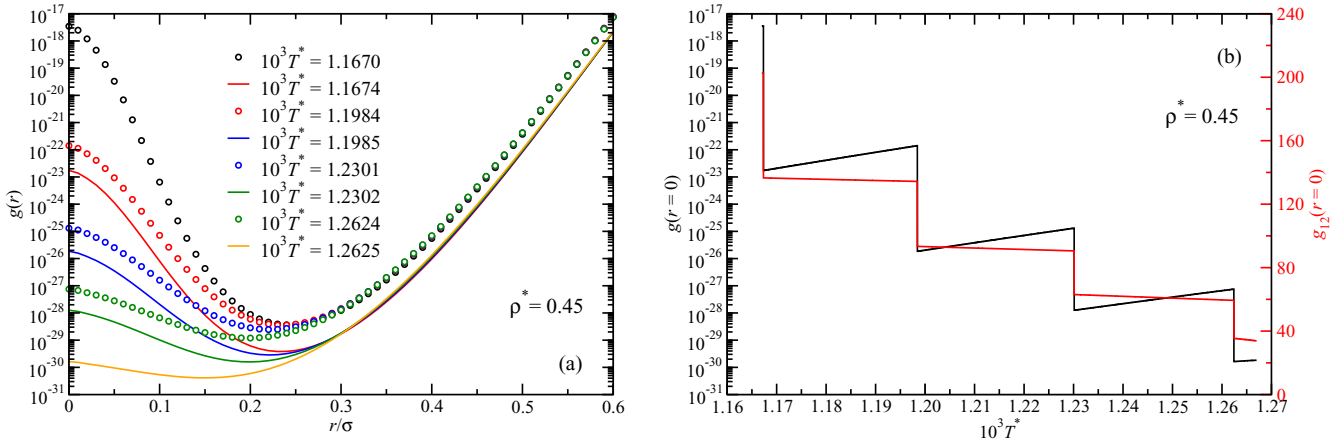

FIG. 6. (a) Small-r behavior of the glass phase $g(r)$ at density $\rho^* = 0.45$ for various temperatures listed above. Open circles denote the highest temperature associated with a given stripe and continuous lines the lowest temperature associated with that stripe. Identical colors signal that the data belong to the same stripe. (b) The values of $g(r = 0)$ (black line, vertical axis to the left) and of the inter-replica RDF $g_{12}(r = 0)$ (red line, vertical axis to the right) as functions of temperature for $\rho^* = 0.45$, across different stripes.

GCM features, within the range of explored parameters, two distinct glassy states separated by a critical isochore, as shown in Fig. 4.

IV. INTERPARTICLE CORRELATIONS IN THE QUANTIZED GLASS

We now turn to the structure of the pair correlations of the continuous and quantized glasses, to gain more insight into the mechanisms of the discreteness of the glassiness in the latter. Figure 5(a) shows the evolution of $g(r)$ of the continuous glass at $\rho^* = 0.30$ across a range of temperatures identical to those shown in Fig. 5(b) for $\rho^* = 0.45$, covering five stripes of the quantized glass in the latter case. The same figure also shows the average number of neighbors up to a separation r, given by $n(r) = 4\pi\rho \int_0^r x^2 g(x)dx$, focusing on the quantity $n(r_{\rm min})$, i.e., at the position of the first minimum of $g(r)$. In Fig. 5(a), the $g(r)$ of the continuous glass evolves continuously as the temperature grows and the quantity $n(r)$ remains essentially unaffected, since all dashed curves in Fig. 5(a) collapse on each other. Moreover, in that case we find $n(r_{\rm min}) \cong 13$, the typical coordination number of a dense, amorphous substance. For the quantized glass, Fig. 5(b), no change is observed for values of temperature within a given stripe (not shown) but clear jumps occur upon crossing stripes. Furthermore, $n(r)$ changes markedly at the crossings of stripes, while the values $n(r_{\rm min})$ are now considerably higher, spanning a range $15.5 \lesssim n(r_{\rm min}) \lesssim 16.5$. Within the small range of temperatures spanning five stripes, the quantized glass reduces its coordination by roughly one particle, while being considerably overcoordinated, in contrast to its continuous counterpart.

Although no difference between the RDFs of the quantized glass within a given stripe can be resolved at finite r values, significant changes can be revealed by looking at this quantity at small values of r, as shown in the main plot of Fig. 6(a). Here, in addition to the temperatures shown in Fig. 5(b), and which correspond to the highest T^* in the stripe (open circles), we also show results for the lowest T^* of each stripe (solid lines). The characteristic maximum at $r = 0$, pointing to the existence of close pairs of particles or clusters in the glass, undergoes a significant drop as the threshold between two stripes is crossed: a tiny increase in supply of thermal energy is causing dissociation of some of these aggregates. At the same time, significant rearrangements of the (depleted) aggregates take place within a stripe, their fraction increasing again slightly, as also shown in Fig. 6(b) (black lines, left vertical axis). The corresponding inter-replica RDF, $g_{12}(r)$, also shows marked quantization across stripes as well as small variations within any given stripe, as can be seen in Fig. 6(b) (red lines, right vertical axis). The high coordination number of the quantized glass can thus be understood by the existence of close pairs of particles or even higher-order aggregates in the system, a feature possible for bounded potentials but evidently absent in the case of hard core interactions. Upon increasing the density, the occurrence of such aggregates increases as well, as can be seen in Fig. 7.

The effect of the quantization on the structure factors $S(q)$ of the glass is shown in Fig. 8. Here a striking crossover can be seen, from a continuous behavior at long wavelengths,

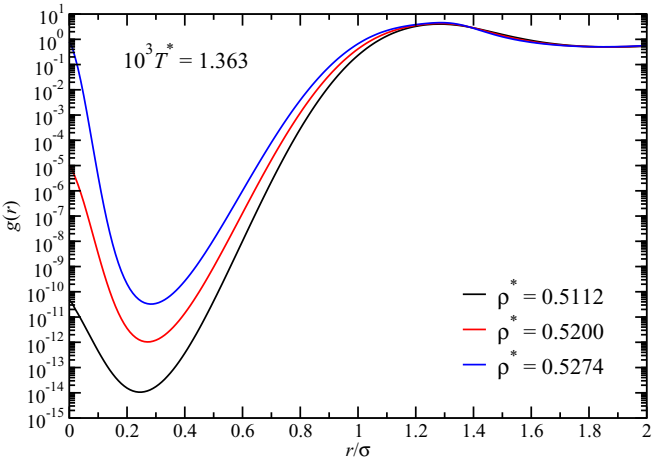

FIG. 7. Small-r behavior of the glass RDF $g(r)$ at reduced temperature $T^* = 1.363 \times 10^{-3}$ for three densities ρ^* listed above.

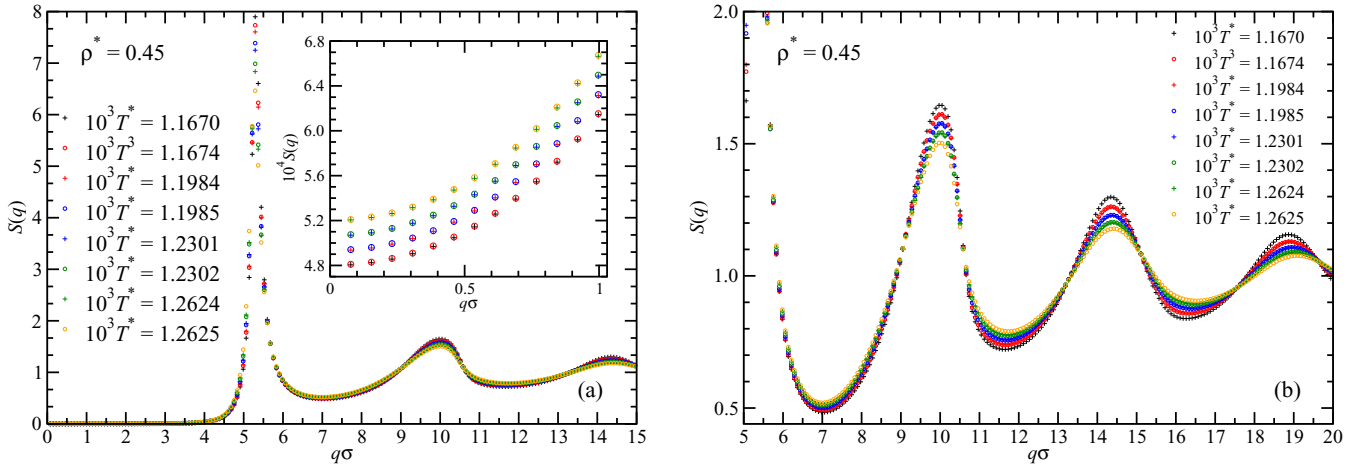

FIG. 8. (a) Main plot: the glass structure factor $S(q)$ at density $\rho^* = 0.45$ for various temperatures listed on the left. Crosses denote the highest temperature associated with a given stripe and open circles the lowest temperature associated with that stripe. Identical colors signal that the data belong to the same stripe. Inset: zoom of the main plot at low q values; for the sake of clarity, the quantity $10^4\ S(q)$ is plotted on the vertical axis. (b) The structure factor for large values of the wave number q.

$q\sigma \lesssim 1$, to a quantized behavior at short wavelengths, $q\sigma \gtrsim 6$. In more detail, we plot in Fig. 8 the structure factors along the isochore $\rho^* = 0.45$, spanning the same range of temperatures as in Fig. 5(b), which covers three fully quantized stripes as well as the highest temperature at the end of the stripe preceding the first full one and a partial stripe after the last one, at the end of which the glass melts. We adopt the same color code as in the rest of the paper, using now full circles of a given color to denote the lowest temperature of a given stripe and crosses of the same color to denote the highest temperature of the same stripe. Colors change upon moving into a new stripe. By construction, the highest temperature of stripe i is infinitesimally lower than the lowest temperature of stripe $i + 1$.

As can be seen in the main plot of Fig. 8(a), the behavior of the glass structure factor in the vicinity of the main peak is neither continuous nor quantized. In the former case, the data from $T^*_{\mathrm{max},i}$ and $T^*_{\mathrm{min},i+1}$ would be practically indistinguishable whereas, in the latter case, that would hold for all data corresponding to the same stripe; neither is true near $q\sigma \approx 5$. As the inset of Fig. 8(a) shows, the continuous scenario materializes at long wavelengths, $q\sigma \lesssim 1$: the colors mix, whereas symbols of the same color are separated by a gap. The compressibility of the glass is a continuous function of temperature along any isochore, despite the fact that we are in the quantized glass regime. Exactly the opposite behavior occurs at short wavelengths, $q\sigma \gtrsim 6$, as shown in Fig. 8(b). Here, the colors demix and all data for the same stripe fall on top of each other, the gaps now separating different stripes. These characteristics support the interpretation of the structural changes presented above for the quantized glasses, as local rearrangements and cluster breakups bring about abrupt changes at short, but not at long wavelengths.

V. CONCLUSIONS

In summary, by combining the HNC integral equation with the replica method, we predict, in addition to a reentrant fluid-glass transition observed at low density, the existence of a transition between a continuous glass at low density and a discretized glass at higher densities in a system of ultrasoft particles interacting via a Gaussian pair potential. The second glass phase exhibits a nonintuitive quantized behavior. We emphasize that the occurrence of local aggregates in the glass phase differs from the recently reported cluster-glass transitions in different models of ultrasoft particles [38–41]. Indeed, in the latter cases the interactions belong to the so-called $Q^{\pm}$ class [7], for which cluster formation is an equilibrium phenomenon, whereas the GCM interaction at hand is a Q^+ potential for which no clusters form at equilibrium. Accordingly, the emergence of a quantized glass is an out-of-equilibrium effect, underlined by the fact that its occurrence is associated with the existence of a local maximum of the glass RDF at $r = 0$. Since a reentrant glass transition has been detected in recent experiments on metallic glasses [42], a quantized glass phase in ultrasoft colloids remains yet to be observed experimentally.

ACKNOWLEDGMENTS

We thank S. Prestipino for providing us with the data from Ref. [19] shown in Fig. 1 as well as M. Camargo (Cali) and V. Sposini (Vienna) for helpful discussions.

[1] P. N. Pusey and W. van Megen, Phase behavior of concentrated suspensions of nearly hard colloidal spheres, Nature (London) **320**, 340 (1986).

[2] C. N. Likos, Soft matter with soft particles, Soft Matter **2**, 478 (2006).

[3] P. J. Yunker, K. Chen, M. D. Gratale, M. A. Lohr, T. Still, and A. G. Yodh, Physics in ordered and disordered colloidal matter composed of poly(n-isopropyl acrylamide) microgel particles, Rep. Prog. Phys. **77**, 056601 (2014).

[4] D. Vlassopoulos and M. Cloître, Tunable rheology of dense soft deformable colloids, Curr. Opin. Colloid Interface Sci. **19**, 561 (2014).

[5] S. Srivastava, L. A. Archer, and S. Narayanan, Structure and Transport Anomalies in Soft Colloids, Phys. Rev. Lett. **110**, 148302 (2013).

[6] A. Lang, C. N. Likos, M. Watzlawek, and H. Löwen, Fluid and solid phases of the Gaussian core model, J. Phys.: Condens. Matter **12**, 5087 (2000).

[7] C. N. Likos, A. Lang, M. Watzlawek, and H. Löwen, Criterion for determining clustering versus reentrant melting behavior for bounded interaction potentials, Phys. Rev. E **63**, 031206 (2001).

[8] B. M. Mladek, D. Gottwald, G. Kahl, M. Neumann, and C. N. Likos, Formation of Polymorphic Cluster Phases for a Class of Models of Purely Repulsive Soft Spheres, Phys. Rev. Lett. **96**, 045701 (2006).

[9] E. Stiakakis, N. Jung, N. Adžić, T. Balandin, E. Kentzinger, U. Rücker, R. Biehl, J. K. G. Dhont, U. Jonas, and C. N. Likos, Self assembling cluster crystals from DNA based dendritic nanostructures, Nat. Commun. **12**, 7167 (2021).

[10] F. H. Stillinger, Phase transitions in Gaussian core system, J. Chem. Phys. **65**, 3968 (1976).

[11] F. H. Stillinger and T. A. Weber, Amorphous state studies with the Gaussian core model, J. Chem. Phys. **70**, 4879 (1979).

[12] F. H. Stillinger, Duality relations for the Gaussian core model, Phys. Rev. B **20**, 299 (1979).

[13] P. J. Flory and W. R. Krigbaum, Statistical mechanics of dilute polymer solutions. 2, J. Chem. Phys. **18**, 1086 (1950).

[14] A. Y. Grosberg, P. G. Khalatur, and A. R. Khokhlov, Polymeric coils with excluded volume in dilute-solution – the invalidity of the model of impenetrable spheres and the influence of excluded volume on the rates of diffusion-controlled intermacromolecular reactions, Makromol. Chem. Rapid Commun. **3**, 709 (1982).

[15] A. A. Louis, P. G. Bolhuis, J. P. Hansen, and E. J. Meijer, Can Polymer Coils be Modeled as "Soft Colloids"?, Phys. Rev. Lett. **85**, 2522 (2000).

[16] A. A. Louis, P. G. Bolhuis, and J. P. Hansen, Mean-field fluid behavior of the Gaussian core model, Phys. Rev. E **62**, 7961 (2000).

[17] P. G. Bolhuis, A. A. Louis, J. P. Hansen, and E. J. Meijer, Accurate effective pair potentials for polymer solutions, J. Chem. Phys. **114**, 4296 (2001).

[18] I. O. Götze, H. M. Harreis, and C. N. Likos, Tunable effective interactions between dendritic macromolecules, J. Chem. Phys. **120**, 7761 (2004).

[19] S. Prestipino, F. Saija, and P. V. Giaquinta, Phase diagram of the Gaussian-core model, Phys. Rev. E **71**, 050102(R) (2005).

[20] A. Ikeda and K. Miyazaki, Thermodynamic and structural properties of the high density Gaussian core model, J. Chem. Phys. **135**, 024901 (2011).

[21] A. Ikeda and K. Miyazaki, Glass Transition of the Monodisperse Gaussian Core Model, Phys. Rev. Lett. **106**, 015701 (2011).

[22] A. Ikeda and K. Miyazaki, Slow dynamics of the high density Gaussian core model, J. Chem. Phys. **135**, 054901 (2011).

[23] J. C. Pamies, A. Cacciuto, and D. Frenkel, Phase diagram of Hertzian spheres, J. Chem. Phys. **131**, 044514 (2009).

[24] H. Jacquin and L. Berthier, Anomalous structural evolution of soft particles: Equilibrium liquid state theory, Soft Matter **6**, 2970 (2010).

[25] T. R. Kirkpatrick and P. G. Wolynes, Connections between some kinetic and equilibrium theories of the glass transition, Phys. Rev. A **35**, 3072 (1987).

[26] T. R. Kirkpatrick and P. G. Wolynes, Stable and metastable states in mean-field Potts and structural glasses, Phys. Rev. B **36**, 8552 (1987).

[27] T. R. Kirkpatrick, D. Thirumalai, and P. G. Wolynes, Scaling concepts for the dynamics of viscous liquids near an ideal glassy state, Phys. Rev. A **40**, 1045 (1989).

[28] M. Mézard and G. Parisi, Statistical physics of structural glasses, J. Phys.: Condens. Matter **12**, 6655 (2000).

[29] J.-M. Bomont, J.-P. Hansen, and G. Pastore, Revisiting the replica theory of the liquid to ideal glass transition, J. Chem. Phys. **150**, 154504 (2019).

[30] C. N. Likos, B. M. Mladek, D. Gottwald, and G. Kahl, Why do ultrasoft repulsive particles cluster and crystallize? Analytical results from density-functional theory, J. Chem. Phys. **126**, 224502 (2007).

[31] J.-P. Hansen and I. R. McDonald, *Theory of Simple Liquids with Applications to Soft Matter*, 4th ed. (Academic Press, Amsterdam, 2013); J.-M. Bomont, Recent advances in the field of integral equation theories: Bridge functions and applications to classical fluids, Adv. Chem. Phys. **139**, 1 (2008).

[32] W. Götze, *Complex Dynamics of Glass-Forming Liquids* (Oxford University Press, New York, 2009).

[33] L. Berthier, A. J. Moreno, and G. Szamel, Increasing the density melts ultrasoft colloidal glasses, Phys. Rev. E **82**, 060501(R) (2010).

[34] F. Camerin, N. Gnan, J. Ruiz-Franco, A. Ninarello, L. Rovigatti, and E. Zaccarelli, Microgels at Interfaces Behave as 2D Elastic Particles Featuring Reentrant Dynamics, Phys. Rev. X **10**, 031012 (2020).

[35] G. Foffi, F. Sciortino, P. Tartaglia, E. Zaccarelli, F. Lo Verso, L. Reatto, K. A. Dawson, and C. N. Likos, Structural Arrest in Dense Star-Polymer Solutions, Phys. Rev. Lett. **90**, 238301 (2003).

[36] W. Kauzmann, The nature of the glassy state and the behavior of liquids at low temperatures, Chem. Rev. **43**, 219 (1948).

[37] J.-M. Bomont, J.-P. Hansen, and G. Pastore, Reflections on the glass transition, in *Advances in the Computational Sciences*, edited by E. Schwegler, B. M. Rubinstein, and S. B. Libby (World Scientific, Singapore, 2017).

[38] D. Coslovich, M. Bernabei, and A. J. Moreno, Cluster glasses of ultrasoft particles, J. Chem. Phys. **137**, 184904 (2012).

[39] D. Coslovich and A. Ikeda, Cluster and reentrant anomalies of nearly Gaussian core particles, Soft Matter **9**, 6786 (2013).

[40] R. Miyazaki, T. Kawasaki, and K. Miyazaki, Cluster Glass Transition of Ultrasoft-Potential Fluids at High Density, Phys. Rev. Lett. **117**, 165701 (2016).

[41] R. Miyazaki, T. Kawasaki, and K. Miyazaki, Slow dynamics coupled with cluster formation in ultrasoft-potential glasses, J. Chem. Phys. **150**, 074503 (2019).

[42] Q. Du, X. Liu, H. Fan, Q. Zeng, Y. Wu, H. Wang, D. Chatterjee, Y. Ren, Y. Ke, P. M. Voyles, Z. Lu, and E. Ma, Reentrant glass transition leading to ultrastable metallic glass, Mater. Today **34**, 66 (2020).